OPEN ACCESS

Dispersion interactions and reactive collisions of ultracold polar molecules

New Journal of Physics
The open-access journal for physics

Dispersion interactions and reactive collisions of ultracold polar molecules

Svetlana Kotochigova
Department of Physics, Temple University, Philadelphia, PA 19122-6082, USA
E-mail: skotoch@temple.edu

New Journal of Physics **12** (2010) 073041 (16pp)
Received 7 March 2010
Published 29 July 2010
Online at http://www.njp.org/
doi:10.1088/1367-2630/12/7/073041

Abstract. Progress in ultracold experiments with polar molecules requires a clear understanding of their interactions and reactivity at ultralow collisional energies. Two important theoretical steps in this process are the characterization of interaction potentials between molecules and the modeling of the reactive scattering mechanism. Here, we report on the *ab initio* calculation of isotropic and anisotropic van der Waals interaction potentials for polar KRb and RbCs colliding with each other or with ultracold atoms. Based on these potentials and two short-range scattering parameters, we then develop a single-channel scattering model with flexible boundary conditions. Our calculations show that, at low temperatures (and in the absence of an external electric field), the reaction rates between molecules or between molecules and atoms have a resonant character as a function of the short-range parameters. We also find that both the isotropic and anisotropic van der Waals coefficients have significant contributions from dipole coupling to excited electronic states. Their values can differ dramatically from those solely obtained from the permanent dipole moment. A comparison with recently obtained reaction rates of fermionic $^{40}K^{87}Rb$ shows that the experimental data cannot be explained by a model where the short-range scattering parameters are independent of the relative orbital angular momentum or partial wave.

Contents

1. Introduction

Recent advances in creating ultracold polar molecules in the lowest rovibrational ground state [1, 2] have created a new scientific playground for studying quantum phenomena that govern collisions and interactions between molecules at low temperatures. Some key theoretical insights into the dipolar character of these interactions have already been developed over the last few years [3]–[9]. It was shown that dipole–dipole forces can be quite strong and may give rise to complex many-body physics in cold polar gases. Molecules with dipole moments, which interact via very long-range dipolar forces when oriented in an external electric field, can form strongly correlated condensed matter-like systems, realize effective spin models and create field-linked states [9]–[12].

Currently, there is also significant interest in the investigation of scattering properties of ultracold molecules. It is expected that such properties will be very different when molecules are held in optical dipole traps or when held in individual sites of an optical lattice. Holding molecules in individual sites of an optical lattice prevents them from approaching each other and allows dipole–dipole forces to play a dominant role in interactions between polar molecules [13, 14]. Intriguingly, in lower dimensional systems, where tight confinement along one or more spatial directions is applied, dipole forces can be engineered to be non-destructive or repulsive and collective effects are predicted [15]–[18]. For example, Gorshkov *et al* [17] have suggested a technique that decreases inelastic collisional rates and enhances elastic collisional rates using a combination of external electric and microwave fields in a two-dimensional (2D) lattice.

In a 3D trapping environment, molecules can scatter freely. Generally, polar molecules are expected to be very fragile to the destructive nature of these collisions. There is experimental evidence for the significant role that such collisions play in defining molecular lifetimes [19]–[23]. The physical origin of this loss is rovibrational relaxations and reactive collisions, both of which occur at short range, when the molecules are close together. An understanding and quantitative description of these collisions might help define the conditions under which an ultracold molecular system is long lived. Furthermore, learning about the short-range region will help us to unravel the role of reactivity in ultracold collisions.

The effect of reactivity on the molecular lifetime at ultracold temperatures, with a few exceptions [23, 24], remains largely unexplored. References [25]–[28] are devoted to theoretical developments towards a full quantum dynamics calculation of reactive collisions with cold molecules. The quantum mechanical description of reactions is challenging due to the complex nature of the differential equations and boundary conditions as well as difficulties in generating potential surfaces of sufficient quality for three- and four-atomic systems. The most successful theories are associated with light atom–diatom systems [29]–[31] that are of astrophysical

interest, and can be Stark decelerated or cooled with a buffer gas. Recently, the extensive quantum scattering calculations in [25, 32, 33] have shown a significant influence of the so-called 'virtual states' in the entrance channel of the collision complex.

The interaction between molecules without an external electric field is dominated by the second-order dipole–dipole interaction. This is a dispersive van der Waals force. For zero electric field, the diagonal matrix elements of the dipole–dipole interaction are zero. At low temperatures, quantum mechanical effects play a prominent role in the molecular scattering from such short- to medium-ranged interaction potentials and are crucial for the description of the interplay between inelastic and elastic collisional rates. The present study explores the isotropic and anisotropic contributions to the dispersion interactions for rotationless $J = 0$ and slowly rotating $J = 1$ polar molecules and introduces a scattering model of ultracold polar alkali–metal molecules valid for rotationless molecules. For rotationless molecules, the dispersion potential is isotropic.

We use a characteristic length scale to distinguish between the dispersion and short-range interaction regions. The short-range boundary, which defines the 'lower limit' of the scattering model, is described by $C_6^{\rm iso}/R_{\rm sr}^6 \ll 2B_e$, where $C_6^{\rm iso}/R_{\rm sr}^6$ is the isotropic dispersion potential and B_e is the rotational constant of the ground state molecule. The short-range separation $R_{\rm sr}$ must be smaller than the isotropic van der Waals length $R_6 = (2\mu C_6^{\rm iso}/\hbar^2)^{1/4}$, where μ is the reduced mass of the molecules. An accurate estimate of these characteristic length scales for KRb and RbCs will be given below.

Our scattering model is an extension of the theory developed in the papers [34, 35]. Here, we modified this scattering theory by making the short-range boundary conditions more flexible by assuming that not all molecules that penetrate to short range will be lost. This allows us to introduce two short-range parameters linked to the rovibrational structure of exit reaction channels. Recently, a model based on quantum defect theory has been introduced in [24], which accounts for the short-range interactions by connecting a complex valued or optical potential to the van der Waals potential.

We calculate the molecule–molecule and atom–molecule van der Waals coefficients by integrating products of the dynamic polarizabily over imaginary frequencies. Unlike for atom–atom interactions, molecular interactions depend on their rotational and vibrational state and can have contributions from transitions within the ground state potential as well as from the electronically excited spectrum. For polar molecules, the former contribution is nonzero, even for levels with a well-defined angular momentum, whereas the excited-state contribution can be significant.

This paper is organized as follows. In section 2, we describe the theory of dispersion interaction isotropic and anisotropic potentials between molecules and molecules with atoms. The numerical potentials and van der Waals coefficients are obtained for the $J = 0$ and 1 X $^1\Sigma^+$ ground state of KRb and RbCs as a function of its vibrational quantum number and presented in section 3. Section 4 gives the basics of our scattering model for rotationless molecules and provides examples of the inelastic scattering rates for ultracold colliding molecules. Lastly, section 5 summarizes and concludes the present research.

2. Dispersion potentials for the molecular interaction

We describe the dispersion interaction potential between molecules A and B, each in a rovibrational level $|{\rm X}, vJM\rangle \equiv |i, M\rangle$ of their X electronic ground state, by assuming that the

molecules are far apart and their wavefunctions do not overlap. Here, the magnetic quantum number M is the projection along a laboratory fixed coordinate system of their total angular momentum $\vec{J}$ and i describes all other quantum labels. Their energy E_i only depends on the label i and not on M. These assumptions allow us to use a (degenerate) second-order perturbation theory similar to that described in [36]. For two molecules, the matrix elements of the dispersion potential between the product states $|i_A, M_A; i_B, M_B\rangle \equiv |i_A, M_A\rangle|i_B, M_B\rangle$ and $|i_A, M'_A; i_B, M'_B\rangle$ with different projection quantum numbers but the same angular momenta J_A and J_B are

$$U_{\rm disp}(\vec{R}) = -\sum_{\substack{S_A\neq i_A, M_A \\ S_B\neq i_B, M_B}} \frac{\langle i_A, M_A; i_B, M_B|V_{dd}|S_A; S_B\rangle\langle S_A; S_B|V_{dd}|i_A M'_A; i_B, M'_B\rangle}{E_{S_A}+E_{S_B}-(E_{i_A}+E_{i_B})}, \tag{1}$$

where the sums S_A and S_B are over all electronic, rovibrational, continuum states of molecules A and B, respectively, restricted to states with energy $E_{S_A}+E_{S_B}\neq E_{i_A}+E_{i_B}$. The operator $V_{\rm dd}$ is the dipole–dipole interaction Hamiltonian [36]

$$V_{\rm dd}(\vec{R}) = -\sqrt{30}\sum_{m_1 m_2 m}\begin{pmatrix}1 & 1 & 2\\ m_1 & m_2 & m\end{pmatrix} d^A_{1m_1} d^B_{1m_2}\frac{C_{2m}(\hat{R})}{R^3}, \tag{2}$$

where d^A and d^B are the two rank-1 spherical dipole operators of the molecules and $\vec{R}$ is the separation between and orientation of the two molecules with respect to a laboratory axis. The $\begin{pmatrix}\cdots\\ \cdots\end{pmatrix}$ is a Clebsch–Gordan coefficient and $C_{lm}(\hat{R})$ is the modified spherical harmonic function [37]. Inserting equations (2) into (1) and after a number of transformations following [36], we find that the dispersion potential is the sum of the isotropic $U_{\rm disp,iso}(\vec{R})$ and anisotropic $U_{\rm disp,aniso}(\vec{R})$ potentials, which can be expressed in terms of the molecular dynamic polarizability tensor at imaginary frequency, $\alpha^{A/B}(\mathrm{i}\omega)$, of molecules A and B.

We find an isotropic $U_{\rm disp,iso}(\vec{R})$ potential

$$U_{\rm disp,iso}(R) = -\frac{C_6^{\rm iso}}{R^6}\delta_{M_A,M'_A}\delta_{M_B,M'_B} - \frac{C_{6,22}^{\rm iso}}{R^6}\langle i_A, M_A; i_B M_B|T_{0,0}(2,2)|i_A, M'_A; i_B M'_B\rangle, \tag{3}$$

where the rank-l tensor operator $T_{l,m_l}(k, p)$ is defined by

$$\begin{aligned}\langle i_A, M_A; i_B, M_B|T_{l,m_l}(k, p)|i_A, M'_A; i_B, M'_B\rangle &= \frac{1}{N_l(k, p)}\sum_{qr}\langle lm_l|kpqr\rangle\\ &\times\langle J_A M_A|J_A k M'_A q\rangle\langle J_B M_B|J_B p M'_B r\rangle\end{aligned} \tag{4}$$

and the normalization $N_l(k, p) = \langle l0|kp00\rangle\langle J_A J_A|J_A k J_A 0\rangle\langle J_B J_B|J_B p J_B 0\rangle$, such that the operator $\langle\ldots|T_{lm_l}(k, p)|\ldots\rangle$ is one for the stretched state $|i_A, M_A\rangle = |i_A, M'_A\rangle = |X, vJ_A J_A\rangle$ and $|i_B, M_B\rangle = |i_B, M'_B\rangle = |X, vJ_B J_B\rangle$. Here, $\langle j_3 m_3|j_2 j_1 m_2 m_1\rangle$ is a Clebsch–Gordan coefficient. Consequently,

$$\begin{aligned}C_6^{\rm iso} &= \frac{3}{\pi}\int_0^\infty \mathrm{d}\omega\langle i_A, J_A|\bar{\alpha}^A(i\omega)|i_A, J_A\rangle\langle i_B, J_B|\bar{\alpha}^B(i\omega)|i_B, J_B\rangle,\\ C_{6,22}^{\rm iso} &= \frac{3}{45\pi}\int_0^\infty \mathrm{d}\omega\langle i_A, J_A|\Delta\alpha^A(i\omega)|i_A, J_A\rangle\langle i_B, J_B|\Delta\alpha^B(i\omega)|i_B, J_B\rangle,\end{aligned}$$

where, for each molecule A and B, $\bar{\alpha} = (\alpha_{xx}+\alpha_{yy}+\alpha_{zz})/3$ and $\Delta\alpha = \alpha_{zz}-(\alpha_{xx}+\alpha_{yy})/2$ are given in terms of diagonal x, y, and z components of the polarizability tensor at imaginary frequency. For atoms and diatoms, the polarizability tensor is fully determined by $\bar{\alpha}$ and $\Delta\alpha$.

The anisotropic van der Waals potential is defined by

$$U_{\mathrm{disp,aniso}}(\vec{R}) = \frac{1}{R^6}\sum_{m_l}(-1)^{m_l}C_{2m_l}(\hat{R})\left\{C^{\mathrm{aniso}}_{6,02}\langle i_A, M_A; i_B, M_B|T_{2,-m_l}(0,2)|i_A, M'_A; i_B, M'_B\rangle\right.$$
$$+C^{\mathrm{aniso}}_{6,20}\langle i_A, M_A; i_B, M_B|T_{2,-m_l}(2,0)|i_A, M'_A; i_B, M'_B\rangle$$
$$\left.+C^{\mathrm{aniso}}_{6,22}\langle i_A, M_A; i_B, M_B|T_{2,-m_l}(2,2)|i_A, M'_A; i_B, M'_B\rangle\right\}$$

and the van der Waals coefficients are

$$C^{\mathrm{aniso}}_{6,02} = -\frac{1}{\pi}\int_0^\infty \mathrm{d}\omega\langle i_A, J_A|\bar{\alpha}^A(i\omega)|i_A, J_A\rangle\langle i_B, J_B|\Delta\alpha^B(i\omega)|i_B, J_B\rangle,$$
$$C^{\mathrm{aniso}}_{6,20} = -\frac{1}{\pi}\int_0^\infty \mathrm{d}\omega\langle i_A, J_A|\Delta\alpha^A(i\omega)|i_A, J_A\rangle\langle i_B, J_B|\bar{\alpha}^B(i\omega)|i_B, J_B\rangle,$$
$$C^{\mathrm{aniso}}_{6,22} = \tfrac{2}{7}C^{\mathrm{iso}}_{6,22}.$$

In our framework, the x, y and z components of the diagonal dynamic polarizability at imaginary frequency are determined as

$$\langle i, M|\alpha_{nn}(i\omega)|i, M\rangle = \frac{1}{\epsilon_0 c}\sum_{S\neq i,M}\frac{(E_S - E_i)}{(E_S - E_i)^2 - (\mathrm{i}\hbar\omega)^2}\times|\langle S|\vec{d}\cdot\hat{n}|i, M\rangle|^2, \tag{5}$$

where $\hat{n}$ is the unit vector along the $n = x$, y, and z directions, i, M and S denote rovibrational wave functions of a single molecule and $\langle S|\vec{d}|i, M\rangle$ are matrix elements of permanent or transition electronic dipole moments. Equation (5) includes a sum over the dipole transitions to the rovibrational levels within the ground-state potential as well as to the rovibrational levels of electronically excited potentials. Contributions from scattering or continuum states of the electronic potentials are also included. Finally, c is the speed of light and ϵ_0 is the electric constant.

In summary, we have found various contributions to the long-range van der Waals potential. They are characterized by their angular momentum dependence. In particular, the term proportional to C^{iso}_6 is independent of magnetic projections and the relative orbital angular momentum between the molecules. The term proportional to $C^{\mathrm{iso}}_{6,22}$ induces coupling between the magnetic projections of the two molecules without affecting the relative orbital angular momentum. Finally, the three C^{aniso}_6 contributions do cause mixing between magnetic projections and relative orbital angular momentum. Note that the coefficients $C^{\mathrm{iso}}_{6,22}$ and $C^{\mathrm{aniso}}_{6,22}$ will be of the same order of magnitude. Both are proportional to a product of two $\Delta\alpha$. Dispersion terms proportional to the spherical harmonic $C_{lm}(\hat{R})$ for $l > 2$ also exist. We do not consider them here as they are smaller.

3. van der Waals coefficients of polar molecules

This section describes our results for the van der Waals coefficients C^{iso}_6 and C^{aniso}_6 between two polar KRb dimers and two RbCs dimers. These molecules are prepared in rovibrational states of the ground $X^1\Sigma^+$ potential and are of interest for ongoing ultracold experiments [1, 2, 23, 38]. We have used the results of electronic structure calculations [39]–[41] for potential energies, permanent and transition electric dipole moments of the KRb and RbCs molecules as a function of internuclear separation. The electronic structure calculations use a

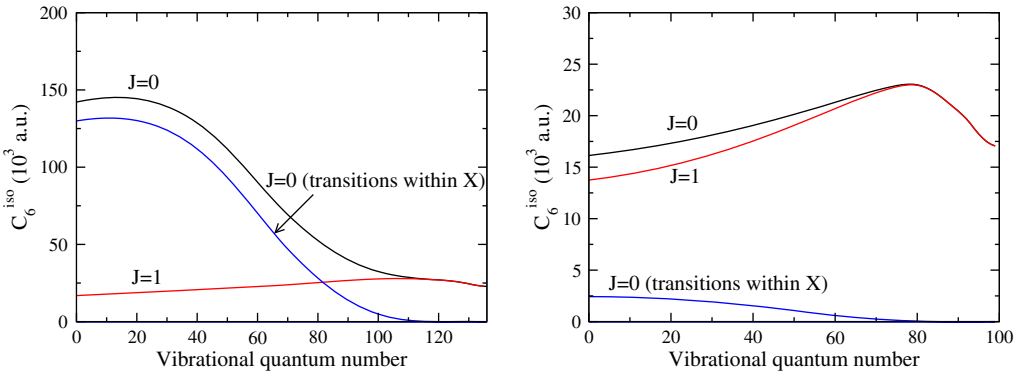

Figure 1. Isotropic molecule–molecule van der Waals coefficients in atomic units for the $J = 0$ and 1 rotational levels of the $X^1\Sigma^+$ ground state of RbCs (left panel) and KRb (right panel) as a function of vibrational quantum number. The curves labeled '$J = 0$ (transitions within X)' correspond to an isotropic van der Waals coefficient where only the contributions from transitions to rovibrational levels of the $X^1\Sigma^+$ potential are included.

non-relativistic *ab initio* multi-reference configuration interaction method. In order to determine experimental observables, we combine these electronic structure calculations with calculations of rovibrational and continuum wavefunctions and energy levels of each potential energy surface included in the determination of the molecular polarizability. These wavefunctions are used to determine vibrationally averaged transition dipole moments between rovibrational levels of the $X^1\Sigma^+$ potential as well as between rovibrational levels of the $X^1\Sigma^+$ and excited potentials. We include transitions from the $X^1\Sigma^+$ potential to the two $^1\Sigma$ and two $^1\Pi$ electronic states dissociating to the first $^2S + ^2P$ and $^2P + ^2S$ excited atomic limits. For alkali–metal atoms, this includes all the effects of the dominant S–P transition. Transitions to higher excited states have small dipole moments and are far detuned.

The isotropic C_6^{iso} coefficients between two molecules both in the $J = 0$ rotational levels of the $X^1\Sigma^+$ ground state potential as a function of vibrational quantum number are shown in figure 1. Comparison of the two panels shows that for the deeply bound $J = 0$ vibrational levels the isotropic coefficient for RbCs is almost an order of magnitude larger than for KRb. This is because for these levels the main contribution to the total value of C_6^{iso} is due to transitions within the ground state potential, which to good approximation is equal to $d_v^4/(6B_v)$ [42], where d_v and B_v are the vibrationally averaged permanent dipole moment and rotational constant of level v, respectively. The permanent dipole moment of RbCs is twice as large as that of KRb, while B_v is almost half the size [2, 39, 41]. The permanent dipole moment of both molecules rapidly decreases to zero with v and the $X^1\Sigma^+$ contribution to the van der Waals coefficient follows this trend. Consequently, for the highly excited vibrational levels, the C_6^{iso} are solely determined by transitions to electronically excited states. In fact, for KRb the excited state contribution plays a dominant role for all v.

Figure 1 also shows the $J = 1$ isotropic dispersion coefficients. These are independent of the projection quantum number M. In this case, the contributions from the transitions from $J = 1$ to $J = 0$ and 2 within the ground state potential have opposite sign and nearly cancel each other. As a result, the value of C_6^{iso} is close to or equal to the value obtained by only including the

Table 1. van der Waals coefficients in atomic units for the interaction between two molecules in the $v = 0$, $J = 0$ and 1 rovibrational levels of the $X^1\Sigma^+$ potential as well as between such a molecule and an atom. The uncertainty in the coefficients is 5%.

	C_6^{iso}		$C_{6,20}^{aniso}$		$C_{6,22}^{aniso}$	
System	$J = 0$	$J = 1$	$(J, M) = (1, 0)$	$(J, M) = (1, \pm 1)$	$(J, M) = (1, 0)$	$(J, M) = (1, \pm 1)$
KRb + KRb	16 133	13 749	2569	−1285	−43	−11
RbCs + RbCs	142 129	16 865	1443	−2886	−630	−157
KRb + Rb	7 696	7 686	1428	−714		
KRb + K	6 905	6 896	1278	−639		
RbCs + Rb	7 326	7 274	798	−399		
RbCs + Cs	8 479	8 416	929	−465		

excited state contributions. The dispersion coefficient is weakly dependent on v. The isotropic values for the $v = 0$ vibrational level of the $X^1\Sigma^+$ state of KRb and RbCs are given in table 1.

The $J = 0$ and 1 dispersion coefficients are the same when they are solely determined by transitions to electronically excited states. This is because rotational energy splittings are negligible compared to electronic excitation energies and the rotational energy dependence of E_{S_A} and E_{S_B} in equation (1) can be neglected. Alternatively, this independence follows from a simple atomistic model for the dispersion coefficient of weakly bound molecules. The molecular electronic wave functions are then to good approximation products of atomic electronic wave functions and the molecule–molecule dispersion coefficient reduces to a sum of atom–atom dispersion coefficients, which do not depend on the rotational state of the molecule. In fact, for RbCs + RbCs, we find that $C_6^{iso} \to 2C_6(\mathrm{RbCs}) + C_6(\mathrm{Rb}_2) + C_6(Cs_2) = 22\,868$ au for large v using the well-characterized Rb + Rb, Rb + Cs and Cs + Cs dispersion coefficients [43]. This value is in good agreement with our results. Similar agreement is found for C_6^{iso} of the interacting KRb molecules based on the values of C_6 from [43].

The collisions between two $J = 1$ molecules are anisotropic. Once molecules are prepared in the specific state characterized by M, the interaction energy can depend on the relative orientation of the two molecules. In fact, the anisotropic interaction can change the projection quantum numbers. Figure 2 (left panel) shows our results for the anisotropic $C_{6,02}^{aniso}$ coefficient as a function of vibrational quantum number for $J = 1$ rotational sublevels, $M = 0$ and $M = \pm 1$, of the $X^1\Sigma^+$ ground state of KRb and RbCs. The anisotropy for RbCs changes sign as a function of v due to competing contributions from the ground and excited states. In both cases, $C_{6,02}^{aniso}$ goes to zero for highly excited vibrational levels. For these collisions, we have $C_{6,20}^{aniso} = C_{6,02}^{aniso}$.

Our predicted isotropic van der Waals C_6^{iso} coefficients for the interaction between KRb molecules have been used in theoretical models [23, 24] to successfully describe the loss rate constant $\mathcal{K}$ observed in a JILA experiment as a function of temperature [23]. The anisotropic C_6^{aniso} coefficients can be used for describing collisions between molecules in nonzero J rotational states. Our estimate shows that an experimentally accessible external electric field of $2\,\mathrm{kV\,cm^{-1}}$ will induce a $\approx$50 MHz splitting between $M = 0$ and $M = \pm 1$ components of $J = 1$ rotational state of KRb. The anisotropic interaction terms, for example, with coefficient $C_{6,02}^{aniso} \approx 2500$ au, will then cause a reorientation of the magnetic sublevels for separations less than $80a_0$ and will contribute to the loss of molecules from the trap.

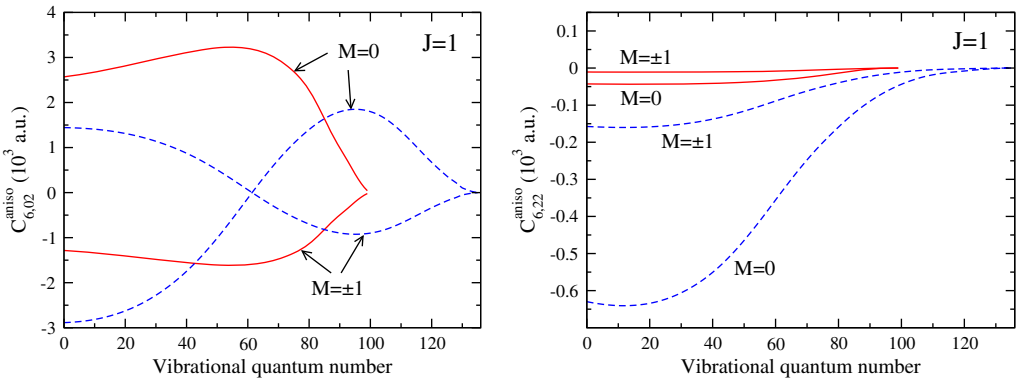

Figure 2. Anisotropic van der Waals coefficients $C^{\text{aniso}}_{6,02}$ (left panel) and $C^{\text{aniso}}_{6,22}$ (right panel) in atomic units as a function of vibrational quantum number for two molecules in $J = 1$ rotational levels of the $X^1\Sigma^+$ ground state of KRb (solid lines) and RbCs (dashed lines). The coefficient is shown for both $M = 0$ and 1. The coefficient for $M = 0$ follows from the one for the stretched state $M = 1$ by evaluation of the tensor T_{lm_l} in equation (4).

We also determined the coefficients $C^{\text{iso}}_{6,22}$ and $C^{\text{aniso}}_{6,22}$. For rotationless $J = 0$ molecules, both coefficients are zero. The right panel of figure 2 shows $C^{\text{aniso}}_{6,22}$ for $J = 1$ as a function of vibrational quantum number. These values are an order of magnitude smaller than the contributions discussed so far. The anisotropic coefficients for both molecules in the $v = 0\, X^1\Sigma^+$ state are given in table 1.

It was observed in [19]–[23] that the lifetime of both Feshbach and deeply bound polar molecules decreases when they are in the presence of ultracold atoms. This suggests that collisions between atoms and molecules play a role in limiting the molecule lifetime. These losses are due to relaxation of rovibrational or hyperfine degrees of freedom that have enough kinetic energy to remove both molecules and atoms from an external optical or magnetic trap. Another possible loss channel is an ultracold chemical reaction. To understand these losses, we determine the isotropic and anisotropic van der Waals coefficients for the interaction between a molecule in state $|i_{\text{Mol}}, M_A\rangle$ and an atom in state $|i_{\text{At}}, M_B\rangle$. Again, following [36], the isotropic coefficient is

$$C_6^{\text{AtMol,iso}} = \frac{3}{\pi}\int_0^\infty \mathrm{d}\omega \langle i_{\text{Mol}}, J_A|\bar{\alpha}^{\text{Mol}}(i\omega)|i_{\text{Mol}}, J_A\rangle\langle i_{\text{At}}, J_B|\bar{\alpha}^{\text{At}}(i\omega)|i_{\text{At}}, J_B\rangle, \tag{6}$$

where $\bar{\alpha}^{\text{Mol}}$ and $\bar{\alpha}^{\text{At}}$ are the mean molecular and atomic polarizabilities, respectively. The anisotropic coefficient is

$$C_{6,20}^{\text{AtMol,aniso}} = \frac{1}{\pi}\int_0^\infty \mathrm{d}\omega \langle i_{\text{Mol}}|\Delta\alpha^{\text{Mol}}(i\omega)|i_{\text{Mol}}\rangle\langle i_{\text{At}}|\bar{\alpha}^{\text{At}}(i\omega)|i_{\text{At}}\rangle. \tag{7}$$

The values for $C_{6,22}^{\text{AtMol,iso}}$, $C_{6,02}^{\text{AtMol,aniso}}$ and $C_{6,22}^{\text{AtMol,aniso}}$ are zero as $\Delta\alpha$ is zero for an atom.

Figure 3 shows the isotropic van der Waals coefficients for RbCs and KRb molecules with constituent atoms of Cs, Rb and Rb, K, respectively. It provides evidence that the van der Waals coefficients for both $J = 0$ and 1 are nearly the same. This is due to the fact that the contribution from transitions within the ground state is negligible. The lack of these contributions affects the

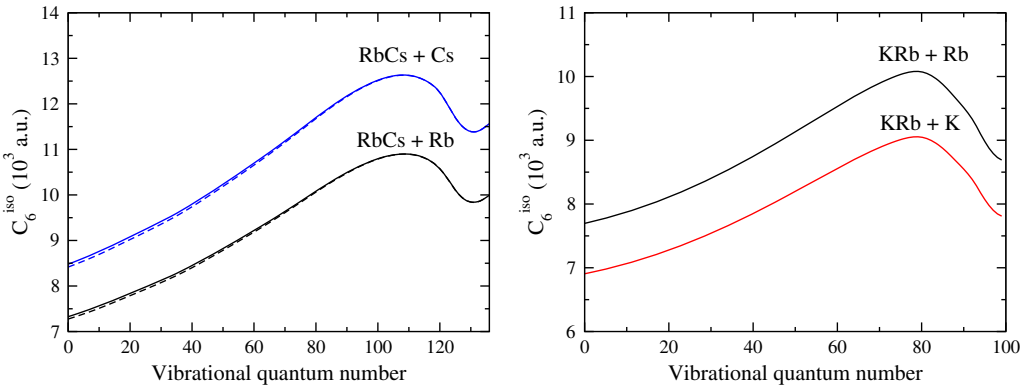

Figure 3. Isotropic van der Waals coefficients in atomic units as a function of vibrational quantum number for the collision between a ground $X^1\Sigma^+$ state RbCs molecule and either an Rb or Cs atom (left panel) and between a KRb molecule and either an Rb or K atom (right panel). Rotational $J = 0(1)$ levels are shown by solid (dashed) lines, respectively. For KRb, the $J = 0$ and 1 C_6^{iso} coefficients are indistinguishable on the scale of a figure.

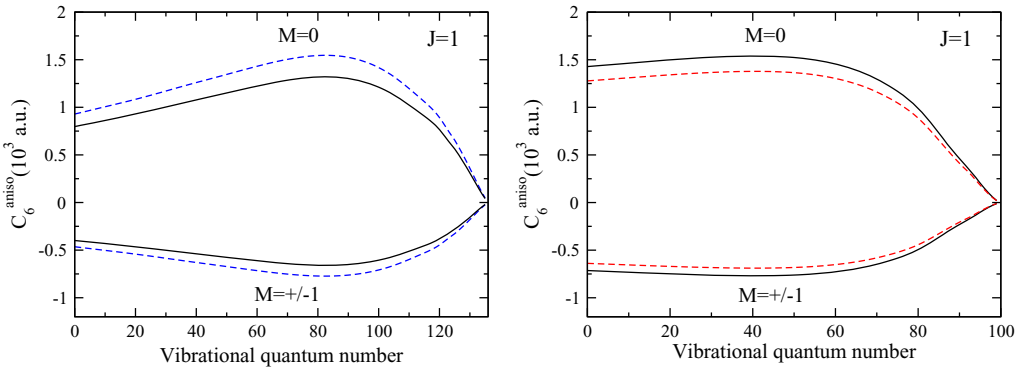

Figure 4. Anisotropic van der Waals coefficients $C_{6,20}^{aniso}$ in atomic units as a function of vibrational quantum number for $J = 1$ rotational $M = 0$ and $M = \pm 1$ sublevels of the $X^1\Sigma^+$ ground state of the RbCs + Rb (solid lines) and RbCs + Cs (dashed lines) interacting systems (left panel) and the KRb + Rb (solid lines) and KRb + K (dashed lines) interacting systems (right panel).

behavior of an anisotropic $C_6^{AtMol,aniso}$ coefficient as well. As is shown in figure 4, the values of the $C_6^{AtMol,aniso}$ for the same projections M have the same sign. Table 1 lists the isotropic and anisotropic values for the $v = 0$ vibrational level of the $X^1\Sigma^+$ state of KRb and RbCs with atoms.

Similar to the molecule–molecule dispersion potential, the van der Waals coefficients for one molecule and one atom are additive for a weakly bound molecule. In other words, the C_6 coefficient for the highly excited vibrational levels can be expressed as a sum of contributions from individual diatoms. For example, $C_6^{RbCs+Rb,iso} \to C_6(RbCs) + C_6(Rb_2) = 10035$ au and $C_6^{RbCs+Cs,iso} \to C_6(RbCs) + C_6(Cs_2) = 12514$ au [43] for weakly bound RbCs molecules. The agreement between the asymptotic values and our numerical calculations is satisfactory. The

same estimate can be carried out for KRb molecules interacting at long distances with K or Rb atoms. This leads to $C_6^{\mathrm{KRb+Rb,iso}} \to C_6(\mathrm{KRb}) + C_6(\mathrm{Rb_2}) = 8965$ au and $C_6^{\mathrm{KRb+K,iso}} \to C_6(\mathrm{KRb}) + C_6(\mathrm{K_2}) = 8171$ au, which agree within a few per cent with the numerical values of figure 3.

4. Reactive collisions of rotationless ultracold polar molecules

The lifetime of ultracold molecules in an optical trap is determined by the inelastic collisional loss rates between these molecules. A collision can change the internal rovibrational state of the molecules as well as induce reactions where the bonds between the atoms are rearranged. For example, for an ultracold KRb gas the reaction $\mathrm{KRb} + \mathrm{KRb} \to \mathrm{K_2} + \mathrm{Rb_2}$ is allowed [23]. Once the molecules are prepared in their absolute ground state, only the reactive process is present.

This section describes our results using a quantum reflection model of the rate coefficient for rotationless $J = 0$ $^{40}\mathrm{K}^{87}\mathrm{Rb}$ and $^{85}\mathrm{Rb}^{133}\mathrm{Cs}$ ground state molecules. The model is based on a modification of the approach developed in [34, 35]. In the absence of an external electric field, these collisions are described by a single radial Schrödinger equation for an isotropic van der Waals potential, since first-order dipole–dipole interaction matrix elements are zero. We solve the Schrödinger equation for $R > R_{\mathrm{sr}}$, where R_{sr} is a short-range separation to be defined below. Two short-range parameters describe the collisional wavefunction when the molecules are 'close' together at $R = R_{\mathrm{sr}}$. As we will show, this boundary condition models the physics or reactivity for $R < R_{\mathrm{sr}}$ and 'partially' inelastic events can occur. The short-range parameters can depend on the rovibrational state of the molecules. The isotropic van der Waals coefficients are taken from table 1. It should be noted that collisions of two $J = 1$ molecules cannot be described by this model. The anisotropic van der Waals contributions will couple relative partial waves, leading to a set of coupled Schrödinger equations. This falls outside the scope of the current paper. Recently, the $J = 0$ model with a different treatment of the short-range interactions was used in [24] for the collisions between KRb molecules.

We use the van der Waals potential to determine the validity of the model and estimate characteristic length scales to distinguish between the dispersion and short-range interaction regions. The range of the isotropic van der Waals potential is defined as $R < R_6 \equiv \sqrt[4]{2\mu C_6^{\mathrm{iso}}/\hbar^2}$, where μ is the reduced molecular mass [44]. For $v = 0$, $J = 0$ KRb and RbCs molecules, this separation is $\approx 300a_0$ and $500a_0$, respectively. The short-range R_{sr} is defined by $C_6^{\mathrm{iso}}/R_{\mathrm{sr}}^6 \approx 2B_v$, where B_v is the rotational constant of the ground state molecule. For shorter separations, the energy of the dispersion potential is much larger than the rotational energy and collisional interactions can mix rotational states. Such mixing falls outside the scope of our single channel description. We find values for R_{sr} between $50a_0$ and $80a_0$ for both molecules. Hence, $R_{\mathrm{sr}} \ll R_6$. In fact, $C_6^{\mathrm{iso}}/R_{\mathrm{sr}}^6$ is much larger than collision energies of interest as well as the centrifugal potential $\hbar^2 l(l+1)/(2\mu R_{\mathrm{sr}}^2)$ between molecules. The quantum number l is the partial wave between the molecules or one molecule and one atom.

Our model involves scattering of rotationless molecules in the potential $-C_6^{\mathrm{iso}}/R^6 + \hbar^2 l(l+1)/(2\mu R^2)$ for $R > R_{\mathrm{sr}}$. The contribution for partial wave l and projection m to the inelastic rate coefficient is given by

$$K_{lm}^{\mathrm{loss}}(E) = v\frac{\pi}{k^2}\sum_{\alpha \neq i} |S_{i\alpha}(E, lm)|^2 = v\frac{\pi}{k^2}(1 - |S_{ii}(E, lm)|^2), \tag{8}$$

where $E = \hbar^2 k^2/(2\mu)$ is the collision energy and v is the relative velocity. The scattering S matrix elements $S_{i\alpha}(E, lm)$ describe the transmission and reflection amplitudes from the initial

state i of colliding molecules and atoms to a final state α with either molecules in different rovibrational states or with a different bond. The sum over α excludes the initial state. Flux conservation or the unitarity of the S matrix allows us to rewrite the loss rate coefficient in terms of the diagonal S matrix element, S_{ii}. At ultracold temperatures, only a few partial waves l contribute as, for higher l, the centrifugal barrier prevents the molecules from approaching each other and K_{lm}^{loss} rapidly goes to zero.

The scattering S matrix is calculated from the radial Schrödinger equation

$$\left(-\frac{\hbar^2}{2\mu}\frac{\mathrm{d}^2}{\mathrm{d}R^2} - \frac{C_6^{\mathrm{iso}}}{R^6} + \frac{\hbar^2}{2\mu}\frac{l(l+1)}{R^2}\right)\psi_{lm}(R) = E\psi_{lm}(R)$$

at collision energy E with the boundary condition

$$\psi_{lm}(R) = A(\mathrm{e}^{+\mathrm{i}[y-\pi/4]} - \zeta_{lm}(E)\mathrm{e}^{2\mathrm{i}\delta_{lm}(E)}\mathrm{e}^{-\mathrm{i}[y-\pi/4]}) \tag{9}$$

at $R = R_{\mathrm{sr}} \ll R_6$, $y = (R/R_6)^{-2}/2$ and A is a normalization constant [44]. The exponents $\mathrm{e}^{\pm\mathrm{i}[y-\pi/4]}$ can be recognized as WKB solutions of a van der Waals potential at zero collision energy. The short-range amplitude $\zeta_{lm}(E)\mathrm{e}^{2\mathrm{i}\delta_{lm}(E)}$ and thus the real parameters $\zeta_{lm}(E)$ and $\delta_{lm}(E)$ are not known *a priori*. They can only be determined from the chemical bonding between the three or four atoms. However, once they are known, the boundary condition uniquely specifies the solution of the Schrödinger equation. Flux conservation requires that $0 \leqslant \zeta_{lm} \leqslant 1$, where $\zeta_{lm} = 0$ corresponds to the case where no flux is returned from the short range and $\zeta_{lm} = 1$ corresponds to the case where everything is reflected back. The phase δ_{lm} describes the relative phase shift of the flux that returns from $R < R_{\mathrm{sr}}$.

The van der Waals potential is the largest energy scale at $R = R_{\mathrm{sr}}$ and, consequently, we initially assume that both $\zeta_{lm}(E)$ and $\delta_{lm}(E)$ are independent of collision energy E, partial wave l and projection m. The validity of these approximations can only be tested by comparison with experimental data. We will do so with the data on KRb loss rate coefficients from [23].

In the limit $R \to \infty$, the wavefunction approaches

$$\psi_l(R) \to \mathrm{e}^{-\mathrm{i}(kr-l\pi/2)} - S_{ii}(E, lm)\mathrm{e}^{\mathrm{i}(kr-l\pi/2)}, \tag{10}$$

where $S_{ii}(Elm)$ is the diagonal S matrix element required for equation (8). In order to determine the relationship between $\zeta_{lm}\mathrm{e}^{2\mathrm{i}\delta_{lm}}$ and $S_{ii}(E, lm)$, we solve the Schrödinger equation analytically in the limit $R_{\mathrm{sr}} \to 0$ using the solutions from [45]. Alternatively, the Schrödinger equation can be solved numerically.

The left panel of figure 5 shows the total loss rate coefficient summed over l and m for collisions between fermionic $^{40}\mathrm{K}^{87}\mathrm{Rb}$ molecules in the $v = 0$, $J = 0$ rovibrational state of the $\mathrm{X}^1\Sigma^+$ potential as a function of the short-range parameters ζ and δ at a collision energy of $E/k_{\mathrm{B}} = 350\,\mathrm{nK}$. For this figure, we assume that $\zeta_{lm} \equiv \zeta$ and $\delta_{lm} \equiv \delta$ are independent of l and m. This rate coefficient can be compared with experimental data on an 'unpolarized' sample of this fermionic KRb molecule with at least two equally populated nuclear-hyperfine states. The right panel shows the loss rate coefficient at $E/k_{\mathrm{B}} = 350\,\mathrm{nK}$ for a 'polarized' sample, where all molecules are in the same nuclear hyperfine state and only odd partial wave scattering is allowed. In fact, for this collision energy only the p wave is significant. The p wave loss rate is much smaller than that for the s wave, since the centrifugal barrier is larger than the 350 nK collision energy and the p-wave loss rate is reduced. We use $C_6^{\mathrm{iso}} = 16\,133$ au for both panels.

The most striking observation of figure 5 is the appearance of resonances in the loss rate. The origin of this behavior is in the interference between the in- and out-going flux for

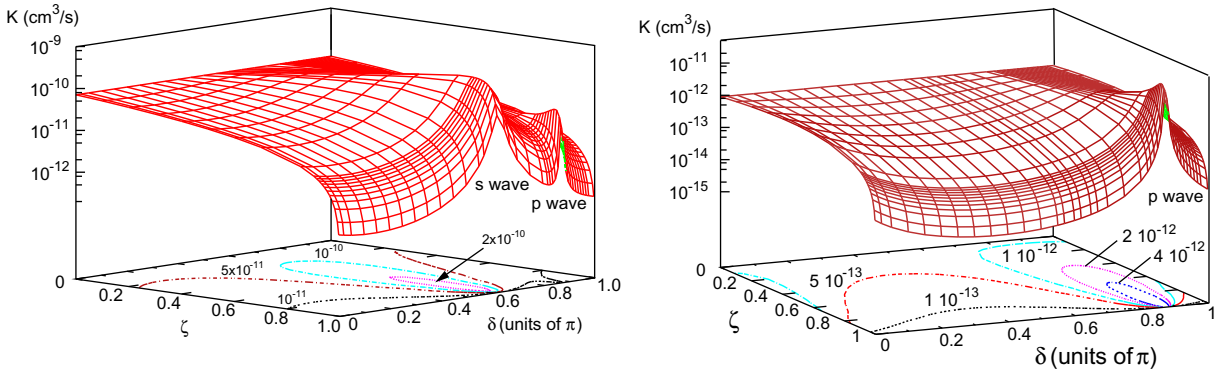

Figure 5. The total inelastic loss rate coefficient for a nuclear spin unpolarized (left panel) and polarized (right panel) sample of $v = 0$, $J = 0$ ^{40}K^{87}Rb molecules in the $X^1\Sigma^+$ potential as a function of the short-range parameters ζ and δ at a collision energy of $E/k_B = 350$ nK. The loss rate of the unpolarized case contains non-negligible contributions from s and p wave contributions. The polarized case only contains odd partial waves.

$R > R_{sr}$. The maximum at ($\zeta \approx 0.8, \delta \approx 0.6\pi$) is due to s-wave collisions and that at ($\zeta \approx 0.95$, $\delta \approx 0.9\pi$) is due to p-wave collisions. In fact, the loss rate is significantly larger than the rate at $\zeta = 0$ when no flux returns from $R < R_{sr}$. (For $\zeta = 0$, the loss rate is independent of δ.) The loss rate can also be much smaller than at $\zeta = 0$. In the limit $\zeta \to 1$, we have $K^{loss} \to 0$. For clarity, this limiting behavior is not shown in the surface plot. If we learn how to change the short-range parameter, we can envision that a significant reduction in the loss rate is possible.

Figure 6 shows a comparison of thermally averaged rate coefficients for ground state ^{40}K^{87}Rb molecules with the experimental observations of Ospelkaus *et al* [23]. The thermal average assumes a Maxwell–Boltzmann distribution. Partial waves up to $l = 3$ are included. In order to obtain the comparison, we assumed that the ζ_{lm} and δ_{lm} are not only independent of partial wave but also independent of collision energy over several kT, where k is the Boltzmann constant.

The experimental rates are $\beta_u = 1.9(4) \times 10^{-10}$ cm^3 s^{-1} for the unpolarized case and $\beta_p = 3.3(7) \times 10^{-12}$ cm^3 s^{-1} for the polarized case at a temperature of $T = 250$ nK. In the experiment, β was extracted from the time dependence of the molecule number density of each nuclear spin state. Consequently, our theoretical loss rate has been multiplied by a factor of two for a polarized sample to account for the loss of two molecules per inelastic collision, and multiplied by one for the unpolarized sample as one atom of each nuclear hyperfine state is lost. Ospelkaus *et al* [23] found that the rates for the polarized and unpolarized sample approximately satisfy the $\beta_u \propto$ const and $\beta_p \propto kT$ Wigner threshold limits as a function of temperature up to $T \approx 1\,\mu$K.

The figure shows regions in the plane (ζ, δ) where the theoretical rate coefficient agrees with the experimental rate coefficients within the uncertainties. One region is for the p-wave-dominated polarized case and one for the s-wave-dominated unpolarized case. The two regions do not overlap. We verified that the uncertainty in the dispersion coefficient does not modify this conclusion. Hence, we conclude that the short-range parameters depend on partial wave l. In fact, figure 6 suggests that it might be sufficient to assume that only the phase δ_{lm} is partial wave dependent. The physical origin of such partial wave dependence must lie in the interferences between the multiple scattering channels that are needed to describe the four-atomic reactive

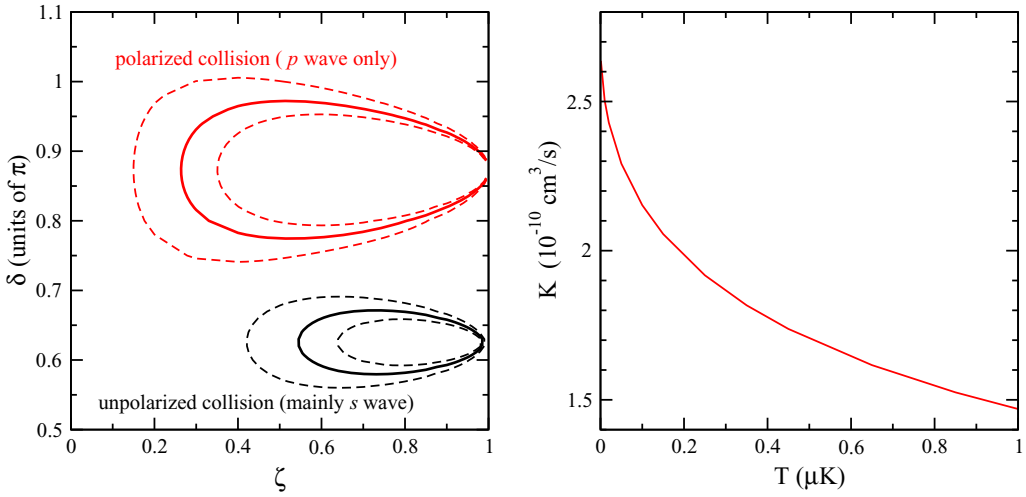

Figure 6. Left panel: bounds on the allowed values of the short-range parameters ζ and δ from the experimental loss rates obtained in [23] for either a nuclear spin unpolarized (black curves) or polarized (red curves) sample of $v = 0$, $J = 0$ ^{40}K^{87}Rb molecules in the $X^1\Sigma^+$ potential at a temperature of $T = 250$ nK. The full lines correspond to pairs of (ζ, δ) where the experimental loss rate agrees with our thermally averaged loss rate. The dashed lines follow from the experimental uncertainty limits. In fact, at a temperature of 250 nK, the measured unpolarized loss rate is $\beta = 1.9(4) \times 10^{-10}$ cm^3 s^{-1}, while that for the polarized case is $\beta = 3.3(7) \times 10^{-12}$ cm^3 s^{-1}. Right panel: the unpolarized loss rate coefficient K of two colliding ^{40}K^{87}Rb molecules as a function of temperature T for $\zeta = 0.55$ and $\delta = 0.63$. For this pair of short-range parameters, the theoretical rate coefficient agrees with the experimental value at a temperature of 250 nK.

scattering process for $R < R_{sr}$. Such a complete description of the reaction requires knowledge of the multi-dimensional electronic potential surface of the four-atomic system. So far, this surface has not been evaluated.

We can compare our results with those of Idziaszek and Julienne [24]. In [24], a model potential with an optical or imaginary term for $R < R_{sr}$ is used to describe the short-range losses. This also leads to a theory with two parameters. The authors were unable to find a simultaneous fit and provided two sets of solutions for the s- and p-wave-dominated loss. We, however, believe that the range of allowed values for the short-range parameters is much larger. In fact, as figure 6 shows, for both s- and p-waves the allowed values fall on an 'ellipse'.

We also note that the temperature dependence of our unpolarized s-wave-dominated loss rate coefficients is non-negligible, even over a temperature range as small as 1 μK. As shown in the right panel of figure 6, the rate coefficient decreases by 50% as the temperature increases from 0 to 1 μK. This observation is true for parameter values where the theory agrees with the experimental observations. Idziaszek and Julienne [24] assume that the thermalized loss rate is independent of temperature and, in effect, quote a zero temperature loss rate.

Figure 7 shows the loss rate coefficient for the collision between two bosonic ^{87}RbCs molecules in the vibrationally excited $v = 1$, $J = 0$ level of the $X^1\Sigma^+$ potential at a collision

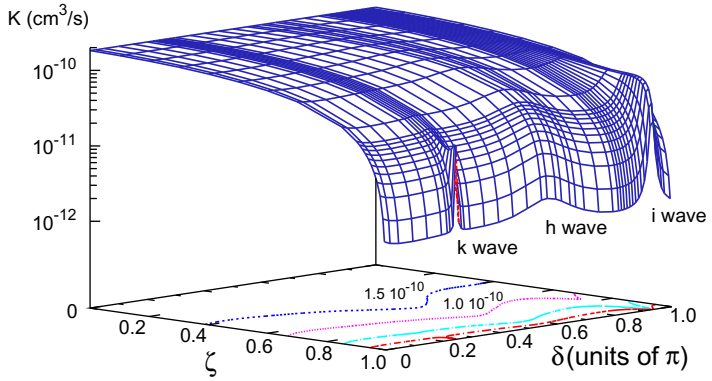

Figure 7. The total inelastic loss rate coefficient for an unpolarized sample of $v = 1$, $J = 0$ ^{87}RbCs molecules in the $X^1\Sigma^+$ potential as a function of the short-range parameters ζ and δ at a collision energy of $E/k_B = 250\,\mu$K. At this collision energy, many partial waves contribute.

energy of $E/k = 250\,\mu$K and $C_6^{iso} = 142\,540$ au. The nuclear hyperfine states are equally populated and partial waves up to $l = 8$ are included. We again assume that the short-range parameters are independent of partial wave. In the figure, maxima or resonances for $l = 5$, 6 and 7 are observed. As can be found from a comparison of the binding energies of the $v = 0$ vibrational levels for the three RbCs, Rb_2 and Cs_2 dimer molecules, chemical reaction at ultracold temperature $RbCs + RbCs \rightarrow Cs_2 + Rb_2$ is endothermic by $\approx 40\,cm^{-1}$ and not energetically allowed. For collisions between $v = 1$ RbCs molecules, the reaction is exothermic. At a $250\,\mu$K collision energy, rate coefficients as large as $2 \times 10^{-10}\,cm^3\,s^{-1}$ can be seen in figure 7. With typical densities in ultracold experiments at about 10^{11} to $10^{12}\,cm^{-3}$, lifetimes as short as 10 ms could be observed.

5. Conclusion

We have performed a theoretical study critical for the physical realization of highly controlled ultracold molecular systems. In particular, we have focused on heteronuclear KRb and RbCs molecules used in ongoing ultracold experiments. Our detailed calculations of the C_6 dispersion coefficients for interactions between molecules or between molecules and atoms helped the experimental [23] and theoretical [24] efforts to quantitatively describe quantum-state controlled chemical reactions.

Analyses of the isotropic and anisotropic interaction potentials of ultracold polar molecules unveiled a significant contribution from dipole coupling to electronically excited states. This leads to a dramatic change in the interaction potentials as compared to previous estimates based solely on the permanent dipole moment.

Our calculations of the scattering between rotationless $J = 0$ polar molecules predict constructive and destructive interferences in the molecular scattering loss rates as a function of short-range phase and amplitude. The long-range dispersion potential between such molecules is purely isotropic. A comparison to recent experimental measurements [23] on the fermionic $^{40}K^{87}Rb$ molecule shows that these short-range parameters must be partial wave dependent. In fact, our calculations suggest that it might be sufficient to assume that only the phase depends

on the partial wave. Such dependence can only be caused by interferences between scattering waves when the molecules are close together. The dependence might even be due to a resonance in the collision.

We also observed that, even at temperatures as low as 1 μK, the energy dependence of the loss rate for unpolarized s-wave-dominated collisions of $^{40}K^{87}Rb$ is non-negligible. At this stage, however, this temperature dependence has not been systematically studied and the experimental uncertainty is large. For the collision of rotationless RbCs molecules at a much higher collision energy of 250 μK, we showed that multiple partial waves can influence the reaction rate. RbCs molecules cannot react when they are prepared in lowest $v = 0$ vibrational level. We studied RbCs molecules prepared in the $v = 1$ level.

Our future plans involve a further elucidation of the reaction process. This requires the generation of a sufficiently accurate three- and four-body potential surface followed by a multi-channel quantum scattering calculation. A multi-channel calculation would also allow us to start making predictions about the effect of an electric field on a reaction.

Acknowledgments

This work was supported by the Air Force Office of Scientific Research MURI award FA 9550-09-1-0588 on Ultracold Molecules. The author acknowledges helpful discussions with Piotr Zuchowski and Eite Tiesinga.

References

[1] Sage J, Sainis S, Bergeman T and DeMille D 2005 *Phys. Rev. Lett.* **94** 203001
[2] Ni K-K, Ospelkaus S, de Miranda M H G, Peer A, Neyenhuis B, Zirbel J J, Kotochigova S, Julienne P S, Jin D S and Ye J 2008 *Science* **322** 231
[3] Baranov M, Dobrek L, Goral K, Santos L and Lewenstein M 2002 *Phys. Scr.* **T102** 74
[4] Goral K, Santos L and Lewenstein M 2002 *Phys. Rev. Lett.* **88** 170406
[5] Ticknor C and Bohn J L 2005 *Phys. Rev.* A **72** 032717
[6] Krems R V 2005 *Int. Rev. Phys. Chem.* **24** 99
[7] Avdeenkov A V, Kajita M and Bohn J L 2006 *Phys. Rev.* A **73** 022707
[8] Rohen S, Bortolotti D C E, Blume D and Bohn J L 2006 *Phys. Rev.* A **74** 033611
[9] Micheli A, Brennen G K and Zoller P 2006 *Nat. Phys.* **2** 341
[10] Lewenstein M 2006 *Nat. Phys.* **2** 309
[11] Avdeenkov A V and Bohn J L 2003 *Phys. Rev. Lett.* **90** 043006
[12] Avdeenkov A V, Bortolotti D C E and Bohn J L 2004 *Phys. Rev.* A **69** 012710
[13] Rom T, Best T, Mandel O, Widera A, Greiner M, Hänsch T W and Bloch I 2004 *Phys. Rev. Lett.* **93** 073002
[14] Thalhammer G, Winkler K, Lang F, Schmid S, Grim R and Hecker-Denschlag J 2006 *Phys. Rev. Lett.* **96** 050402
[15] Büchler H P, Micheli A and Zoller P 2007 *Nat. Phys.* **3** 726
[16] Büchler H P, Demler E, Lukin M, Micheli A, Prokof'ev N, Pupillo G and Zoller P 2007 *Phys. Rev. Lett.* **98** 060404
[17] Gorshkov A V, Rabl P, Pupillo G, Micheli A, Zoller P, Lukin M D and Büchler H P 2008 *Phys. Rev. Lett.* **101** 073201
[18] Pupillo G, Micheli A, Büchler H P and Zoller P 2009 *Cold Molecules: Theory, Experiment, Applications* ed R V Krems, B Friedrich and W C Stwalley (London: Taylor and Francis)
[19] Hudson E R, Gilfoy N B, Kotochigova S, Sage J M and DeMille D 2008 *Phys. Rev. Lett.* **100** 203201

[20] Gaebler J P, Stewart J T, Bohn J L and Jin D S 2007 *Phys. Rev. Lett.* **98** 200403
[21] Zirbel J J, Ni K-K, Ospelkaus S, D'Incao J P, Wieman C E, Ye J and Jin D S 2008 *Phys. Rev. Lett.* **100** 143201
[22] Ospelkaus S, Ni K-K, de Miranda M H G, Neyenhuis B, Wang D, Kotochigova S, Julienne P S, Jin D S and Ye J 2009 *Faraday Discuss.* **142** 351–9
[23] Ospelkaus S, Ni K-K, Wang D, de Miranda M H G, Neyenhuis B, Guéméner G, Julienne P S, Bohn J L, Jin D S and Ye J 2010 *Science* **327** 853
[24] Idziaszek Z and Julienne P S 2009 arXiv:0912.0370v1
[25] Weck P F and Balakrishan N 2006 *Int. Rev. Phys. Chem.* **25** 282
[26] Hutson J M and Soldan P 2007 *Int. Rev. Phys. Chem.* **26** 1
[27] Krems R V, Stwalley W C and Friedrich B 2009 *Cold Molecules: Theory, Experiment, Applications* (London: Taylor and Francis)
[28] Krems R V 2008 *Phys. Chem. Chem. Phys.* **10** 4079
[29] Aldegunde J, de Miranda M P, Haigh J M, Kendrich B K, Sáez-Rábans V and Aoiz F J 2005 *J. Phys. Chem.* A **109** 6200
Aldegunde J, Alvariño J M, de Miranda M P, Sáez Rabanos V and Aoiz F J 2006 *J. Chem Phys.* **125** 133104
[30] Alvariño J M, Aquilanti V, Cavalli S, Crocchianti S, Laganà A and Martínez T 1997 *J. Chem. Phys.* **107** 3339
Aldegunde J, Alvariño J M, De Fazio D, Cavalli S, Grossi G and Aquilanti V 2004 *Chem. Phys.* **301** 251
[31] Tscherbul T V and Krems R V 2008 *J. Chem. Phys.* **129** 034112
[32] Balakrishan N and Dalgarno A 2001 *Chem. Phys. Lett.* **341** 652
[33] Bodo E, Gianturco F A, Balakrishan N and Dalgarno A 2004 *J. Phys. B: Quantum Semiclass. Opt.* **37** 3641
[34] Julienne P S and Mies F H 1989 *J. Opt. Soc. Am.* B **6** 2257
[35] Orzel C, Walhout M, Sterr U, Julienne P S and Rolston S L 1999 *Phys. Rev.* A **59** 1926
[36] Stone A J 1996 *The Theory of Intermolecular Forces* (London: Clarendon)
[37] Brink D M and Satchler G R 1993 *Angular Momentum* (London: Clarendon)
[38] Pilch K, Lange A D, Prantner A, Kerner G, Ferlain F, Nägerl H-C, Grimm R and Chin C 2009 *Phys. Rev.* A **79** 042718
[39] Kotochigova S, Julienne P S and Tiesinga E 2003 *Phys. Rev.* A **68** 022501
[40] Kotochigova S, Tiesinga E and Julienne P S 2009 *New J. Phys.* **11** 055043
[41] Kotochigova S and Tiesinga E 2005 *J. Chem. Phys.* **123** 174304
[42] Barnett R, Petrov D, Lukin M and Demler E 2006 *Phys. Rev. Lett.* **96** 190401
[43] Derevianko A, Babb J F and Dalgarno A 2001 *Phys. Rev.* A **63** 052704
[44] Gao B 2000 *Phys. Rev.* A **62** 050702
[45] Gao B 2009 *Phys. Rev.* A **80** 012702